Journal of Alloys and Compounds 489 (2010) 558–561

Contents lists available at ScienceDirect

Journal of Alloys and Compounds

journal homepage: www.elsevier.com/locate/jallcom

Structural relaxation and serrated flow due to annealing treatments in Zr-based metallic glasses

G.S. Yu [a], J.G. Lin [a,*], W. Li [b,*], Z.W. Lin [b]

[a] Faculty of Material and Photoelectronic Physics, Key Laboratory of Low Dimensional Materials & Application Technology (Ministry of Education), Xiangtan University, Xiangtan 411105, China
[b] School of Chemical and Materials Engineering, Huangshi Institute of Technology, Huangshi 435003, China

ARTICLE INFO

Article history:
Received 3 August 2009
Received in revised form
16 September 2009
Accepted 17 September 2009
Available online 25 September 2009

Keywords:
Alloys
Glasses
Microstructure

ABSTRACT

In this work, the effect of the annealing treatment on the serrated flow in $Zr_{41.2}Ti_{13.8}Cu_{12.5}Ni_{10}Be_{22.5}$ bulk metallic glass was investigated. It was found that the as-cast alloy exhibited a pronounced serration flow, and the critical strain rate, number and displacement of the pop-ins of the serration decreased with the increase in annealing temperature. The decrease in free volume may be responsible for the change of the serration behavior in the annealed samples.

1. Introduction

Bulk metallic glasses (BMGs) have attracted considerable attention due to their unique properties such as high strength and hardness, high fracture toughness, good corrosion resistance, and excellent wear resistance [1,2]. It is well documented that plastic deformation in amorphous alloys at room temperature is accommodated through the development of multiple shear bands, and is highly localized in very thin shear bands, resulting in a very low ductility of the alloys at room temperature. The poor ductility of BMGs may limit their forming or application, therefore, many investigations of deformation, fracture, and shear banding in various BMG alloys. It is generally known that the BMGs have excess free volume, which is defined as “holes” or “voids” and plays a dominant role in the diffusive arrangement of atoms, trapped within the amorphous structure depending on the preparation conditions [3–6]. Annealing of the glasses at temperatures near or below the glass transition temperature (T_g) will result in the annihilation of this additional free volume and the glass gradually relaxes into the more equilibrium state. This structural relaxation may lead to a considerable change in their physical properties [7–11]. The free volume is apparently important parameter as a chain to understand the correlation between the structural characteristics and relevant mechanical properties. However, the mechanism responsible for the embrittlement and especially the change of plastic deformation behavior in metallic glasses due to structural relaxation still need to be identified. Schuh and Nieh [12] recently studied the shear band pop-in phenomenon under different load rates and temperatures using a nanoindenter. They successfully applied the free volume theory for explaining the observed shear band evolution patterns. The serrated flow phenomenon ascribe to the change of free volume. However, it is not clear how the free volume would affect the serrated flow behavior of BMGs yet. In this work, nanoindentation tests were conducted on a metallic glass, $Zr_{41.2}Ti_{13.8}Cu_{12.5}Ni_{10}Be_{22.5}$, in as-cast state and annealed state, aiming at establishing the experimental relationship between the free volume and the serrated flow behavior in a Zr-based metallic glass.

2. Experimental

The $Zr_{41.2}Ti_{13.8}Cu_{12.5}Ni_{10}Be_{22.5}$ BMGs was prepared by sucking the melt into copper mold. The samples were isothermally annealed at 523 K and 573 K for 12 h, and at 593 K and 633 K for 1 h in vacuum, respectively. The amorphous nature was ascertained by X-ray diffraction and differential scanning calorimetry (DSC), and the results have been reported elsewhere [13]. Instrumented nanoindentation experiments were conducted using a Triboindenter. The tests were performed in the load control mode with a maximum load of 8000 μN. Loading rates were chosen to be 2 mN/s, 0.08 mN/s, 0.04 mN/s and 0.02 mN/s, respectively. Scanning electron microscopy (SEM) was used to observe the morphology around the indents.

* Corresponding authors.
E-mail address: wenl@ualberta.ca (W. Li).

0925-8388/$ – see front matter © 2009 Elsevier B.V. All rights reserved.
doi:10.1016/j.jallcom.2009.09.108

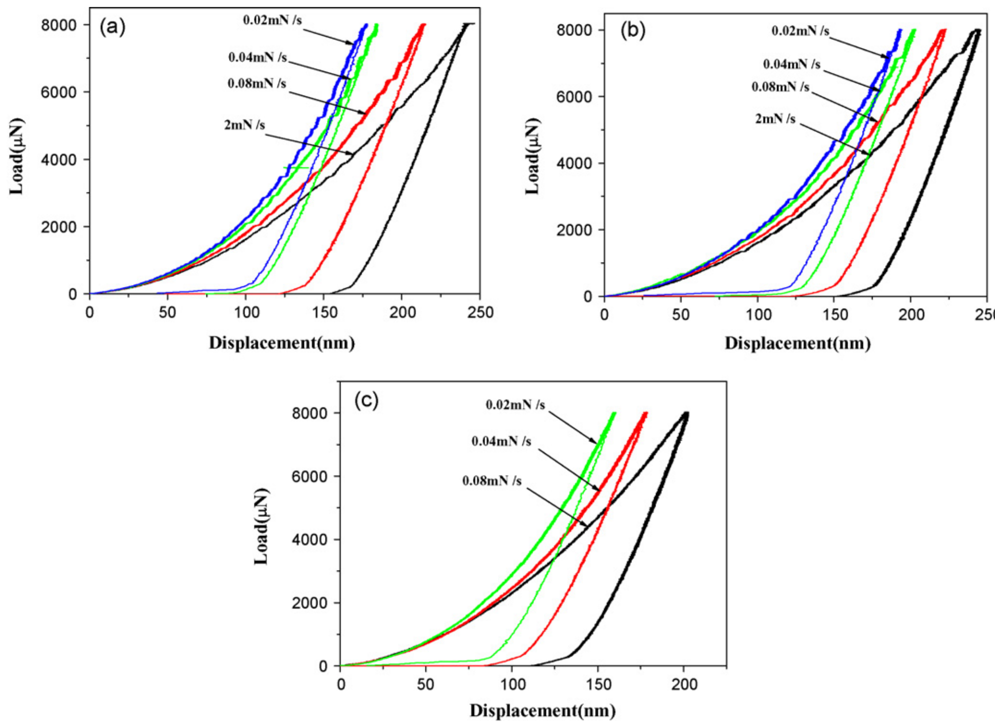

Fig. 1. Typical load–displacement (*P*–*h*) curves during nanoindentation; as-cast sample (a), and sample annealed at 573 K for 12 h (b), and 633 K for 1 h (c).

3. Results and discussions

Fig. 1 shows the load–depth (*P*–*h*) curves of the as-cast sample and the samples annealed at 573 K and 633 K during nanoindentation at the various loading rates. It can be found that the serrated flow not only depends strongly on the loading rate, but also on the annealing temperature. The serrated flow occurred in the as-cast and the sample annealed at 573 K for 12 h at low loading rates, but no distinct serrations can be found in the annealed BMGs (633 K) at the loading rates chosen in the present work. For the as-cast sample, the critical rate is about 0.08 mN/s, while this value decreased to be 0.02 mN/s for the sample annealed at 537 K for 12 h. The serrated flow during nanoindentation has already been observed in many BMG systems, which is attributed to the nucleation and propagation of shear bands underneath the indenter [14,15]. Moreover, the serrated flow was suppressed at high loading rates or the precipitation of crystalline phases, due to the formation multiple shear bands [9]. The present results indicate that the structural relaxation caused by low temperature annealing also lead to the weakness of serration flow during nanoindentation. In order to examine if there is any quantitative differences in the pop-in displacements, Δh, between the as-cast and annealed alloys, the pop-in displacements of the samples at the indentation rate of 0.02 mN/s were calculated, which are presented in Fig. 2. It can be clearly seen that the number and size of the pop-ins gradually decrease with the annealing time. The average Δh is about 85 nm for the as-cast alloy, and it is 60 nm for the sample annealed at 573 K for 12 h. While, after 633 K annealing, no distinct pop-in events can be observed in the sample. It should also be noted that the serrated flow occurred in the as-cast and the sample annealed at 573 K for 12 h at low loading rates, but no distinct serrations can be found in the annealed BMGs (633 K) at the loading rates chosen in the present work. For the as-cast sample, the critical rate is about 0.08 mN/s, while this value decreased to be 0.02 mN/s for the sample annealed at 537 K for 12 h. This proves that the start of the inhomogeneous flow is more sluggish in the annealed samples.

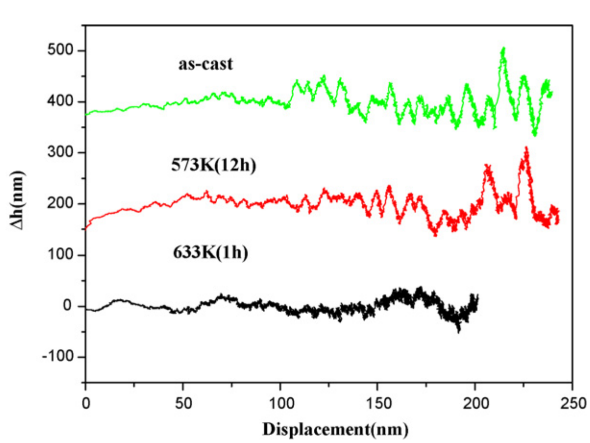

Fig. 2. The displacement of the pop-ins (Δh) in the different samples at the indentation rate of 0.02 mN/s.

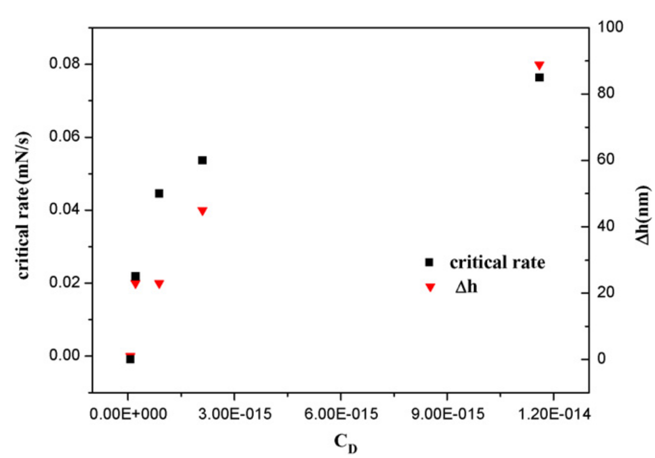

Fig. 3. The correlation of the change of critical rate and Δh with the defect concentration in the BMG.

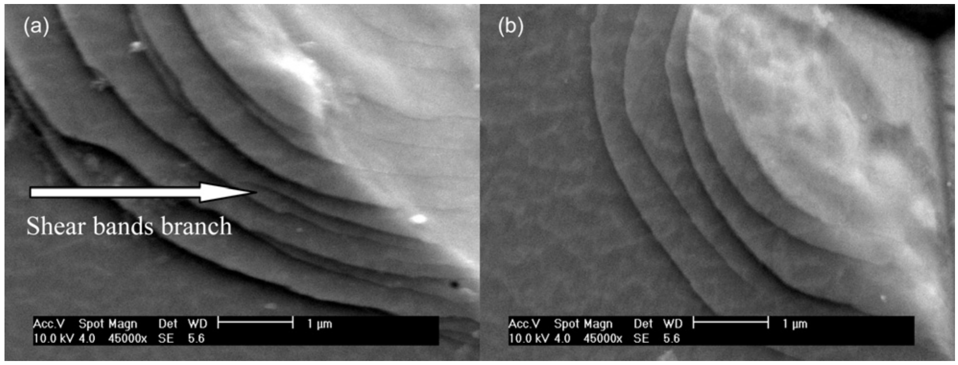

Fig. 4. SEM images of the shear bands of the as-cast sample (a) and the sample annealed at 573 K for 12 h (b).

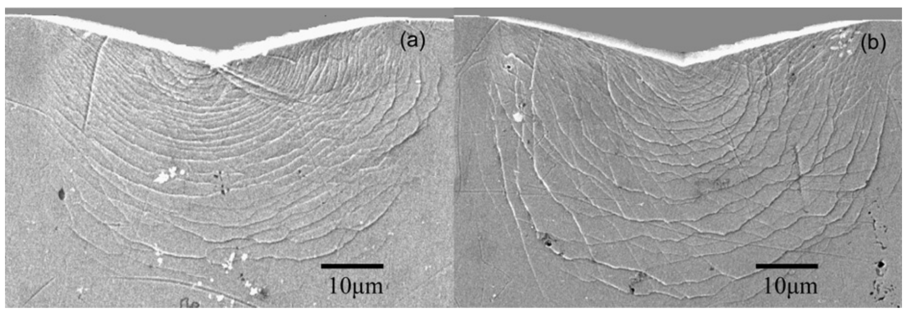

Fig. 5. SEM images of the deformation region underneath a Vickers indenter for the as-cast sample (a) and the sample annealed at 573 K for 12 h (b). The load is 98 N for both samples.

The annealing process at a temperature near the T_g is generally regarded as a structural relaxation process, and the excess volume in the structure will be removed with a sufficient annealing time. The process can be thought to be a result of the free volume influences to the serration behavior. It has been confirmed that the reduction of the free volume associated with the structure relaxation can be accessed on the basis of the DSC testing result [13,16–19]. The defect concentration c_D is utilized to characterize the state of metallic glass and related to the reduced free volume x by $c_D = \exp(-1/x)$. The change in the defect concentration due to the structural relaxation during the annealing progress can be expressed by the differential equation as follows [18]:

$$\frac{dc_D}{dt} = -k_r c_D (c_D - c_D^{eq}) \tag{1}$$

where t denotes time; k_r is a temperature-dependent rate factor for structural relaxation, which has the form of $k_r = k_0 \exp(-E_f/k_B T)$ (k_B is Boltzmann's constant); $c_D^{eq}[c_D^{eq} = \exp(-1/x_{ep})]$ denotes the defect concentration in the metastable equilibrium. The DSC signal can be simulated by using the only fit parameter, initial defect concentration c_D^0, which is calculated to be 1.16×10^{-14}, 2.10×10^{-15}, 8.84×10^{-16}, 2.12×10^{-16}, and 6.70×10^{-17} for the as-cast sample and the samples annealed at 523 K (12 h), 573 K (12 h), 593 K (1 h) and 633 K (12 h), respectively. The changes of the displacement of the pop-ins and the critical rate with the defect concentration are illuminated in Fig. 3. It can be seen that the serrated flow feature strongly depends on the defect concentration, i.e., the free volume. With the decrease of the free volume, the critical rate for the appearance of the serrated flow and the displacement of the pop-ins decrease.

It has been well documented that each serration corresponds to the activation of individual shear banding [8,10,14]. Embrittleness of a metallic glass is related to the excessive propagation of individual shear bands which may reflect in an enlarged serrations during nanoindentation. According to Schuh's microscopic plastic flow equation of metallic glasses [1,14], the shear strain rate can be expressed as

$$\dot{\gamma} = \frac{\dot{\tau}}{\mu} + 2f \exp\left(-\frac{\alpha v^*}{v_f}\right) \sinh\left(\frac{\tau \Omega}{2k_B T}\right) \exp\left(-\frac{\Delta G^m}{k_B T}\right) \tag{2}$$

where $\dot{\gamma}$ is the strain rate and $\dot{\tau}$ is the rate of change of the applied stress; ΔG^m is the activation energy for an atomic jump; f is the jump frequency; T is the temperature; α is a geometrical factor on the order of 1 and Ω is the atomic volume. If the applied shear stress is sufficiently large, the free volume created by the applied shear stress is greater than the annihilation due to diffusion, and thus, the net rate of change of the free volume v_f, is governed by

$$\dot{v}_f = v^* f \exp\left(-\frac{\Delta G^m}{k_B T}\right) \exp\left(-\frac{\alpha v^*}{v_f}\right) \times \left\{\frac{\alpha}{v_f} \frac{2k_B T}{S}\left[\sinh\left(\frac{\tau \Omega}{2k_B T} - 1\right) - \frac{1}{n_D}\right]\right\} \tag{3}$$

where v^* is the critical free volume required for an atomic jump ($\approx 8\,\Omega$); S is a material constant given by $(2/3)\mu(1+\nu/1-\nu)$, ν is Poisson's ratio and μ is the shear modulus; n_D is the number of atomic jumps required to annihilate the free volume v^*. The structural relaxation process is associated with redistribution and reduction of defect concentration. As a result, the nucleation and propagation of shear band become difficult, which is reflected by the increased ΔG^m. According to Eqs. (2) and (3), the values of $\dot{\gamma}$ and v_f decrease with the annealing temperature, and, thus, gives rise to the low the critical strain rate for the shear bands nucleation. This increased critical strain rate is also responsible for the increased time interval between the operations of consequent shear bands in the relaxed samples, which is reflected by less number of serration during nanoindentation (as seen in Figs. 1 and 2). Furthermore, for the relaxed samples with relatively low c_D^0, much more free volume is needed to initiate a shear band. Consequently, a larger volume of the surrounding materials in the relaxed samples should be involved for the aggregation of the free volume compared to the as-cast alloy.

To further understand the relationship between the serrated flow and shear band deformation, the shear band morphologies in the deformation region around the indents of the annealed samples were observed, which are shown in Fig. 4. A number of incomplete circular patterns of shear bands were observed in the pile up area around the indents for the as-cast and the isothermal annealed samples. For the as-cast sample, the density of shear bands was higher than with that in the annealed sample, and some secondary shear band branches were observed as well. By contrast, only primary shear bands were found in the annealed sample. To clearly show the change of the deformation mechanism in the BMGs with the annealing temperature, the underneath deformation morphologies of the typical samples were investigated through Vickers indenter using bonded interface technique (see Fig. 5). Many semi-circular and radial shear bands are observed in the plastic deformation region of the as-cast and annealed samples. It is interesting to find that the as-cast sample shows the fine and dense shear band upset, while the annealed sample (573 K) exhibits the largest shear band upset. This suggests that the nucleation and propagation of shear band is much more difficult in the annealed samples than that in the as-cast sample, which is consistent with the result of nanoindentation test.

4. Conclusions

The effect of the anneal treatment on the serrated flow and shear band features of a Zr-based BMG has been investigated. The critical strain rate for the appearance of the serration, the number of serrations and the displacement of the pop-ins depended strongly on the annealing temperature. The nucleation and propagation of the shear band in the annealed samples became more difficult than that in the as-cast sample. Such experimental results can be attributed to the reduction of free volume in the annealed samples.

Acknowledgements

The authors would like to acknowledge financial support from the National Natural Science Foundation of China (Nos. 10972190 and 10872177), the Hunan Provincial Nature Science Foundation of China (No. 09JJ3086), and State Key Lab of Advanced Metals Materials (No. EG512677781CN).

References

[1] A. Inoue, H.M. Kimura, Mater. Trans. JIM 35 (1994) 85.
[2] C.C. Hays, C.P. Kim, W.L. Johnson, Phys. Rev. Lett. 84 (2000) 2901.
[3] A.S. Argon, et al., Acta Metall. 27 (1979) 47.
[4] C.A. Pampillo, et al., J. Mater. Sci. 10 (1975) 1194.
[5] U. Ramamurty, M.L. Lee, J. Basu, Y. Li, Scr. Mater. 47 (2002) 107.
[6] O. Haruyama, M. Tando, H.M. Kimura, N. Nishiyama, A. Inoue, Mater. Sci. Eng. A 375–377 (2004) 293.
[7] J.J. Lewandowski, P. Lowhaphandu, Philos. Mag. A82 (2002) 3247.
[8] C.A. Schuh, T.G. Nieh, J. Mater. Res. 19 (2004) 46.
[9] J.J. Kim, Y. Choi, S. Surech, A.S. Argon, Science 295 (2002) 654.
[10] B.C. Wei, W.H. Li, T.H. Zhang, L.C. Zhang, Intermetallics 12 (2004) 1239.
[11] W.H. Jiang, M. Atzmon, J. Mater. Res. 18 (2003) 755.
[12] C.A. Schuh, T.G. Nieh, Acta Mater. 51 (2003) 87.
[13] G.S. Yu, et al., Mater. Sci. Eng. A 460–461 (2007) 58.
[14] C.A. Schuh, A.C. Lund, T.G. Nieh, Acta Mater. 52 (2004) 5879.
[15] H.W. Zhang, X.N. Jing, G. Subhash, L.J. Kecskes, R.J. Dowding, Acta Mater. 53 (2005) 3849–3859.
[16] W.J. Wright, R. Sasa, W.D. Nix, Mater. Trans. JIM 42 (2001) 642.
[17] A.L. Greer, et al., Mater. Sci. Eng. A375–377 (2004) 1182.
[18] F. Spaepen, Acta Metall. 25 (1977) 407.
[19] A. van den Beukel, S. Radelaar, Acta Metall. 31 (1983) 419.